Published in final edited form as:
J Bone Miner Res. 2012 March ; 27(3): 563–574. doi:10.1002/jbmr.1474.

Osteocytic Network Is More Responsive in Calcium Signaling than Osteoblastic Network under Fluid Flow

X. Lucas Lu[1,2,+], **Bo Huo**[1,3,+], **Victor Chiang**[1], and **X. Edward Guo**[1,*]

[1]Bone Bioengineering Laboratory, Department of Biomedical Engineering, Columbia University, New York, NY 10027

[2]Department of Mechanical Engineering, University of Delaware, Newark, DE 19716

[3]Institute of Mechanics, Chinese Academy of Sciences, Beijing 100190, P. R. China

Abstract

Osteocytes, regarded as the mechanical sensor in bone, respond to mechanical stimulation by activating biochemical pathways and mediating the cellular activities of other bone cells. Little is known about how osteocytic networks respond to physiological mechanical stimuli. In this study, we compared the mechanical sensitivity of osteocytic and osteoblastic networks under physiological related fluid shear stress (0.5–4 Pa). The intracellular calcium ($[Ca^{2+}]_i$) responses in micro-patterned *in vitro* osteoblastic or osteocytic networks were recorded and analyzed. Osteocytes in the network showed highly repetitive spike-like $[Ca^{2+}]_i$ peaks under fluid flow stimulation, which are dramatically different from those in osteoblastic network. The number of responsive osteocytes in the network remained at a constant high percentage (>95%) regardless of the magnitude of shear stress, while the number of responsive osteoblasts in the network significantly depends on the strength of fluid flow. All spatiotemporal parameters of calcium signaling demonstrated that osteocytic networks are more sensitive and dynamic than osteoblastic networks, especially under low level mechanical stimulations. Furthermore, pathway studies were performed to identify the molecular mechanisms responsible for the differences in $[Ca^{2+}]_i$ signaling between osteoblastic and osteocytic networks. The results suggested that the T-type voltage gated calcium channels (VGCC) expressed on osteocytes may play an essential role in the unique kinetics of $[Ca^{2+}]_i$ signaling in osteocytic networks, while the L-type VGCC is critical for both types of cells to release multiple $[Ca^{2+}]_i$ peaks. The extracellular calcium source, intracellular calcium store in ER, ATP, PGE_2, NO and caffeine related pathways are found to play similar roles in the $[Ca^{2+}]_i$ signaling for both osteoblasts and osteocytes. The findings in this study proved that osteocytic networks possess unique characteristics in sensing and processing mechanical signals.

Keywords

Osteocytes; Osteoblasts; Cell Network; Mechanotransduction; Fluid Flow; Calcium Signaling

[*]Corresponding Author: X. Edward Guo, Ph.D., 351 Engineering Terrace, Mail Code 8904, 1210 Amsterdam Avenue, New York, NY 10027, U.S.A., ed.guo@columbia.edu, Telephone: 212-854-6196, Fax: 212-854-8725.
[+]These authors contributed equally to the work

Disclosure

All authors state that they have no conflicts of interest.

Author's roles: Study design: XEG, and XLL. Study conduct: XLL, BH, and VC. Data analysis: XLL and VC. Data interpretation: XLL, BH, and XEG. Drafting manuscript: XLL. Revising manuscript content: BH, VC, and XEG. Approving final version of manuscript: XLL, BH, VC, and XEG.

Introduction

Osteocytes are the most abundant cells in bone, composing more than 90% of bone cell population (1). Throughout the lacunae-canaliculi system, osteocytes build connections with each other with their numerous dendritic processes, and form an extensive cell network in the mineral matrix (2–4). The elaborate osteocytic networks act as a high efficient sensor in bone for detecting mechanical signals generated by host's daily physical activities. The osteocytic network draws a morphological similarity with neuronal network, suggesting a potential in processing and translating mechanical stimuli. Recent findings showed that the bone adaptation process requires osteocytes to detect mechanical signals *in situ* and integrate the signals into appropriate anabolic or catabolic activities of the bone cell system (3–6). A prominent mechanism for osteocytes to communicate with each other is through the intercellular physical connections. Osteocytes can establish gap junction intercellular communication (GJIC) with each other at the end of long processes as well as cells on the bone surface (mainly lining cells and osteoblasts) and cells in bone marrow (7,8). However, studies showed that osteoblast could also regulate cellular activities in response to mechanical stimuli, *e.g.*, fluid flow can induce prominent calcium responses in osteoblasts or osteoblastic networks (9–12). The key question, which has yet to be investigated, is whether an osteocytic network behaves differently from an osteoblastic network under physiological mechanical environment. The means by which these two types of networks coordinate with each other or harmonize their mechanotransduction activities are thus far poorly understood. The focus of this study, as a first step, was to compare the mechanical sensitivity between osteocytic and osteoblastic networks in terms of intracellular calcium ($[Ca^{2+}]_i$) signaling induced by fluid flow.

Physical loading on bones from daily physical activities can generate fluid flow in the lacunae-canaliculi system and further exert shear stress on bone cell processes and bodies (2). Shear stress generated by fluid flow has been shown to play a critical role in the mechanotransduction process in bone cells and to be able to initiate a cascade of biochemical activities in cells (10,12–15). Analytical modeling predicted that the fluid shear stress on osteocytes is in the range of 0.8~3 Pa (16), while recent imaging techniques estimated that the peak shear stress on osteocyte processes could reach 5 Pa (17). In this study, to compare the sensitivity of osteocytic and osteoblastic network in response to mechanical stimulation, a full range of fluid shear stress under unidirectional steady fluid flow expected to occur during routine human physical activities, *i.e.*, 0.5–4 Pa, will be employed as mechanical stimuli. The unidirectional steady flow was chosen to represent a physiological but unusual mechanical stimulus that is different from the oscillatory flow presumed to occur under cyclic daily activities (14). It is known that bone cells, including both osteocytes and osteoblasts, respond more actively to new patterns or types of mechanical loading. This is a major advantage of using unidirectional flow in this cell comparison study.

Studies have shown that fluid flow can induce consistent oscillations of $[Ca^{2+}]_i$ intensity in bone cells (15,18–20). Calcium signaling is observed as one of the earliest biochemical responses in bone cells under mechanical stimuli and can regulate many downstream signaling events (21–23). For example, blocking extracellular calcium influx or inhibiting the release of calcium from intracellular store can markedly inhibit the mechanically-induced PGE_2 release in osteocytes (24). It has been recently shown that the $[Ca^{2+}]_i$ responses can propagate between neighboring cells, and the calcium wave propagation can act as a critical mechanism for cell-cell communication in bone cell networks (20,25–27). More importantly, the $[Ca^{2+}]_i$ oscillation in osteoblasts has been shown to be dependent on the mechanical loading frequency and magnitude of shear stress (28).

The fluid flow induced elevation of cytosolic calcium mainly comes from two sources: intracellular buffering stores (*e.g.*, endoplasmic reticulum, ER) and the extracellular environment (29–31). The Ca^{2+} exchange between intra- and extracellular environments involves stretch activated ion channels, store operated calcium channels, voltage gated calcium channels (VGCC), and other ligand-gated ion channels (*e.g.*, ATP activated P_2X_7 receptor). A recent study demonstrated that osteoblasts predominantly express L-type VGCC, while osteocytes, in contrast, express T-type VGCCs and a relatively small amount of L-type VGCCs (32). The release of intracellular Ca^{2+} pools such as ER occurs mainly through the inositol trisphosphate (IP_3) pathway. IP_3 can bind to the receptors on the ER leading to a rapid release of Ca^{2+} stored in the ER (33,34). Another type of calcium channel on the reticulum is ryanodine receptor (RyR), the sensitivity of which can be dramatically increased by high caffeine concentration (35). When the cytosolic calcium concentration is elevated to a critical level by intra/extracellular sources, the depleted intracellular calcium stores undergo a rapid reuptake through Ca^{2+}-ATPase. Simultaneously an extrusion of Ca^{2+} across the plasma membrane through Ca^{2+} pumps and Na^+/Ca^{2+} exchanger helps to reduce the $[Ca^{2+}]_i$ intensity to the resting level and prepares cells for the next calcium response (33,36). Previous studies showed that nitric oxide and PGE_2, two essential pathways in bone metabolism, may also be involved in bone cell $[Ca^{2+}]_i$ signaling. Fluid shear stress can prompt the induction of COX-2 protein expression and induce further PGE_2 release in osteocyte-like and osteoblast-like cells (37,38). Nitric oxide modulates $[Ca^{2+}]_i$ signaling via a cyclic guanosine monophosphate (cGMP) dependent pathway (39) or nitrosylation of proteins (40). Moreover, nitric oxide could directly contribute to the $[Ca^{2+}]_i$ release via triggering of an influx pathway that is, in part, responsible for refilling of the internal calcium stores (41). All of these pathways may significantly contribute to the spatial-temporal characteristics of $[Ca^{2+}]_i$ transients in bone cells under mechanical stimulation.

In this study, we hypothesized that the mechano-sensitivity of an osteocytic network is different from that of an osteoblastic network in terms of their spatiotemporal characteristics of $[Ca^{2+}]_i$ responses. Using our novel *in vitro* micro-patterned bone cell networks, we propose to (A) compare the mechano-sensitivity of osteoblastic and osteocytic networks under physiologically relevant mechanical stimuli, (B) examine the spatiotemporal characteristics of $[Ca^{2+}]_i$ signaling in osteoblastic and osteocytic network and their dependence on the stimulation intensity, and (C) investigate the roles of major $[Ca^{2+}]_i$ signaling pathways and identify the potential mechanisms responsible for the difference between osteocytic and osteoblastic networks in their $[Ca^{2+}]_i$ responses. This study represents the first effort to systematically compare the mechano-sensitivity between osteocytes, the so-called “mechanical sensor”, and osteoblasts as two distinctive cell networks.

Materials and Methods

Chemicals

Minimum essential alpha medium (α-MEM), calcium free Dulbecco’s modified eagle medium (DMEM), calcium-free Hank’s balanced salt solution (HBSS), and ATP determination kit were obtained from Invitrogen Corporation (Carlsbad, CA). Fetal bovine serum (FBS), charcoal-stripped FBS, and penicillin/streptomycin (P/S) were obtained from Hyclone Laboratories Inc (Logan, UT). Trypsin/EDTA, octadecanethiol, dimethyl sulfoxide (DMSO), fibronectin, 18α-glycyrrhetinic acid (18α-GA), suramin, caffeine, EGTA, Tetracaine hydrochloride, NNC 55-0396, amlodipine, and thapsigargin were obtained from Sigma-Aldrich Co (St. Louis, MO). N-(2-Cyclohexyloxy-4-nitrophenyl) methanesulfonamide (NS-398) and NG-monomethyl-L-arginine (L-NMMA) were from EMD Chemicals Inc (San Diego, CA).

Cell Culture

Osteocyte-like MLO-Y4 cells (a generous gift from Dr. Lynda Bonewald, University of Missouri-Kansas City, Kansas City, MO) were cultured on type I rat tail collagen (BD Biosciences, San Jose, CA, USA) coated Petri-dish in α-MEM supplemented with 5% FBS, 5% calf serum (CS) and 1% P/S (42). MC3T3-E1 osteoblastic cells were cultured in α-MEM containing 10% FBS and 1% P/S. Cells were maintained at 37°C and 5% CO_2 in a humidified incubator and not allowed to exceed 70–80% confluency in order to maintain the dendritic characteristic of the cell lines.

Bone Cell Network

Micro-contact printing and self-assembled monolayer (SAM) surface chemistry technologies were employed to construct *in vitro* bone cell networks for calcium signaling experiments as described previously (43,44). This technique can precisely control the geometric topology of cell network, unify the intercellular connections for each individual cell, and best mimic native structure of mature bone cell networks. In brief, a grid mesh cell pattern was designed using parameters optimized for MC3T3-E1 and MLO-Y4 cells, respectively. The designed patterns were printed on a chromium mask and then replicated to a master made of positive photoresist (Shipley 1818, MicroChem Corp, Newton, MA) by exposing the master to UV light through the chromium mask. Polydimethylsiloxane (PDMS, *Sylgard 184,* Dow Corning, Midland, MI) was poured on the master and oven cured at 85 °C. Micro-contact printing PDMS stamps with the designed pattern were obtained by lifting off the PDMS from the master surface. To build a bone cell network, the PDMS stamp was dipped into an adhesive SAM (octadecanethiol) and then pressed onto a gold coated glass slide (custom-designed by an E-beam evaporator; SC2000, SEMICORE Inc., Livermore, CA). The stamped glass slide was immediately immersed in a non-adhesive ethylene glycol terminated SAM solution ($HS\text{-}C_{11}\text{-}EG_3$; Prochimia, Sopot, Poland) for at least three hours. A monolayer of EG_3, which can effectively resist protein adsorption and cell adhesion, was formed on areas that were not previously inked with the adhesive SAM. To further improve the cell attachment on the adhesive SAM inked regions, the glass slide was incubated in a 1% fibronectin solution for one hour before cell seeding, where the fibronectin only deposited on the adhesive SAM region. Finally MC3T3-E1 or MLO-Y4 cell suspension was dropped onto the glass slide for one-hour seeding process (approximately 1.0×10^4 cell/cm^2 slide area). The cell seeded slide was cultured for 24 hours before the fluid flow experiment. Fluorescent images of typical well-formed cell networks for each cell type were shown in Figure 1 A&B. Each cell attaches on a round island and connects with four neighboring cells through their dendrites.

Fluid Flow Stimulation and $[Ca^{2+}]_i$ Responses

To indicate $[Ca^{2+}]_i$ signaling, cell networks were incubated in a humidified incubator for 45 minutes with 10 μM Fura-2 AM medium (Molecular Probes, Eugene, OR) and then rinsed with fresh working medium (α-MEM without phenol-red supplemented with 2% FBS and 2% CS) three times. The slide was mounted into a custom-built parallel plate flow chamber for laminar fluid flow stimulation (Fig. 1C). The flow chamber was mounted on an inverted fluorescence microscope (Olympus IX71, Melville, NY) and left undisturbed for 15 minutes, which has been shown to be sufficient for bone cells to recover from disturbance and to generate repetitive $[Ca^{2+}]_i$ responses (45). A magnetic gear pump (SiLog, Micropump, Inc., WA) was connected to the chamber to run the fresh working medium through the chamber with a desired steady flow rate.

The $[Ca^{2+}]_i$ responses of bone cell networks under fluid flow stimulation were recorded with a high-speed CCD camera (ORCA-ER-1394, Hamamatsu Photonics K.K., Hamamatsu City, Japan) for a period of total 10-minutes, one minute for baseline and 9 minutes after the onset

of fluid flow. Fura-2 340 nm/380 nm ratio images were used to obtain the dynamic history of $[Ca^{2+}]_i$ by measuring the average image intensity of each cell using MetaMorph Imaging Software 7.0 (Molecular Devices, Downingtown, PA). The intensity of $[Ca^{2+}]_i$ for each cell was normalized by its corresponding baseline.

Osteocytic and Osteoblastic Networks under Fluid Flow

Cell networks of each cell type were separated into four groups and stimulated with one of the following shear stress on the cell surface: 0.5, 1, 2, and 4 Pa, which were designed to cover the range of *in vivo* fluid flow stress on osteocytes (16,17). Total of eight groups of cell networks were tested in this study, four groups each for MLO-Y4 and MC3T3-E1 cells. The number of tested cell network slides and analyzed cells were summarized in Table 1.

$[Ca^{2+}]_i$ Signaling Pathway Studies

To compare the contribution of major $[Ca^{2+}]_i$ signaling pathways in the responses of osteocytes and osteoblasts, each type of cell networks were divided into eight groups, and the fluid flow experiments were performed with the presence of specific pathway inhibitors in each group. The pathways investigated in this study were schematically illustrated in Fig. 4A. The shear stress of fluid flow was 2 Pa for all groups. Therefore the untreated groups can be adopted from previous flow strength studies. The other seven groups are specified as following: (1) *Extracellular calcium depletion:* In this group, calcium-free DMEM and calcium-free HBSS were used to replace the regular medium in fluid flow tests (99 MC3T3-E1 cells and 66 MLO-Y4 cells analyzed in this group). (2) *ER calcium store depletion*: Cell networks were incubated in 1 μM thapsigargin (TG) medium for 30 min prior to flow. TG depletes calcium from the ER store (46) (90 MC3T3-E1 cells and 111 MLO-Y4 cells). (3) *PGE_2 blocking*: Cell networks were treated with 10 μM NS-398 for 24 hours before the flow study. NS-398 selectively inhibits the COX-2 enzyme activity, which in turn blocks the PGE_2 release (37) (123 MC3T3-E1 cells and 139 MLO-Y4 cells). (4) *NO blocking*: 100 μM L-NMMA was introduced into the cell culture medium one day before seeding the cells on the slides and continuously presented in medium afterwards. L-NMMA inhibits the production of nitric oxide via competitively inhibiting all three isoforms of nitric oxide synthase (NOS) (47) (189 MC3T3-E1 cells and 131 MLO-Y4 cells). (5) *Gap junction blocking*: 75 μM 18α-GA, a reversible gap junction blocker which binds to membrane proteins and causes disassembly of gap junction plaques (48), was supplied in fluid flow medium (49) (61 MC3T3-E1 cells and 125 MLO-Y4 cells) (6) *Extracellular ATP pathway blocking:* 100 μM suramin, a P2 purinergic receptor blocker, was applied to the cell networks 30 minutes before exposing to shear flow (50) (50 MC3T3-E1 cells and 95 MLO-Y4 cells). (7) *Vehicle DMSO control:* Among all the previously employed chemicals, NS-398, 18α-GA, and TG were dissolved into DMSO. Therefore, vehicle control was tested with 0.3% v/v DMSO presented in medium (51 MC3T3-E1 cells and 151 MLO-Y4 cells). The concentrations of above agents were chosen from the relevant literature in bone cells where they have been demonstrated to be effective in inhibiting respective pathways.

Roles of T-type and L-type VGCCs

T-type or L-type VGCC blocker was added into the flow medium 280 seconds after the onset of fluid flow to identify the roles of VGCC in $[Ca^{2+}]_i$ transients of MC3T3-E1 cells and MLO-Y4 cells. NNC 55-0396 (18 μM), a selective inhibitor of T-type Ca^{2+} channel (51), was employed to block the T-type VGCCs, while amlodipine (10 μM) was used to inhibit the L-type VGCCs (52). Four experimental groups were tested in this study with two types of cells and two inhibitors. The experiments were repeated on at least three slides for each individual group.

Data Analysis

The number of responsive cells in each group was evaluated. A cell was defined as responsive to the fluid flow stimulation if it successfully released a calcium spike with a magnitude four times higher than its fluctuations during the period of baseline measurement (11). The number of $[Ca^{2+}]_i$ peaks during the stimulation period were then counted for all the responsive cells. To further quantitatively analyze the spatiotemporal characteristics of the $[Ca^{2+}]_i$ transients, a set of parameters were defined as shown in Fig. 1D. The magnitudes of the first $[Ca^{2+}]_i$ peak were measured and compared between different groups. The time between the onset point of fluid flow and the maximum value of the first responsive spike was defined as 'time to 1st peak', denoted as t_1, to evaluate the responsive speed of cells under various mechanical stimulations. 'Relaxation time of 1st peak' (t_2) was defined as the time it takes for the $[Ca^{2+}]_i$ intensity to drop 50% from first peak magnitude. The time interval and the ratio of magnitudes between the first and second $[Ca^{2+}]_i$ peaks were also reported and compared between all cell groups.

Student t-tests were used to determine significant difference of each parameter (number of peaks, magnitude of 1st peak, time to 1st peak, relaxation time of 1st peak, time between 1st and 2nd peak, and ratio between magnitudes of 2nd and 1st peaks) between MLO-Y4 and MC3T3-E1 cells at a specific stimulation strength. All data are shown as mean ± stand deviation. One-way analysis of variance (ANOVA) with Bonferroni's post hoc analysis was performed to determine statistical differences between mean values of different stimulation strength for each cell type. To determine the correlation between a spatiotemporal parameter and the stimulation strength, a linear regression analysis was performed. The number of $[Ca^{2+}]_i$ peaks were compared between 16 groups using ANOVA with Bonferroni's post hoc analysis to analyze the effects of different pathways. Two-way ANOVA was performed to identify the interaction between two factors, cell type and pathway inhibition. Statistical significance can be observed when $P<0.05$.

Results

The Number of Responsive Cells and Multiple $[Ca^{2+}]_i$ Peaks

A set of typical $[Ca^{2+}]_i$ transients from MLO-Y4 and MC3T3-E1 cells under 2 Pa fluid flow stimulation were shown in Fig. 2A. MC3T3-E1 cells released a strong $[Ca^{2+}]_i$ peak at the onset of flow, which was followed by a few lower peaks during the 9-minute fluid flow stimulation period. A large portion of MLO-Y4 cells, interestingly, tended to demonstrate repetitive, spike-like peaks, the number of which can reach up to 17 during the 9-minute fluid flow stimulation. Thus, it took an MLO-Y4 cell less than 30 seconds to demonstrate a full $[Ca^{2+}]_i$ spike. For the MLO-Y4 cells that released spike-like responses, the magnitudes of $[Ca^{2+}]_i$ peaks tended to be maintained at a constant level, *i.e.*, no declining trend as observed in MC3T3-E1 cells. Under all levels of fluid flow stimulation, few MC3T3-E1 cells demonstrated similar spike-like repetitive $[Ca^{2+}]_i$ transients with these from MLO-Y4 cells.

The number of responsive MLO-Y4 cells under four different fluid flow strength varied between 96–97.2% (Fig. 2B), and no statistical trend was detected between the number of responsive cells and the fluid flow strength. The number of responsive MC3T3-E1 cells increased as the mechanical stimulation intensified, 59% at 0.5 Pa, 84% at 1 Pa, 98% at 2 Pa, and 99% at 4 Pa. Under all fluid flow rates, the average number of $[Ca^{2+}]_i$ peaks of MLO-Y4 cells was significantly higher than that of MC3T3-E1 cells ($P<0.01$) (Fig. 2C). Linear regression analysis showed that the number of peaks for both cell types is positively correlated with fluid flow rate. ANOVA found that the number of peaks of MLO-Y4 cells was statistically different at all stimulation strengths. For MC3T3-E1 cells, no significant

difference was detected between the two groups under 2 and 4 Pa stimulations, and all other groups were significantly different with each other. When fluid stress was 0.5 or 1 Pa, more than 60% MLO-Y4 cells released a single $[Ca^{2+}]_i$ peak, but when shear stress was equal to or higher than 2 Pa, more than 50% of MLO-Y4 cells tended to release 4 or more repetitive $[Ca^{2+}]_i$ peaks. Under all fluid flow rates, more than 40% MC3T3-E1 cells had zero or a single $[Ca^{2+}]_i$ peak, and over 70% cells released 3 or less $[Ca^{2+}]_i$ peaks during a 9-minute fluid flow stimulation under all levels of stimuli (results not shown).

Spatiotemporal Characteristics of $[Ca^{2+}]_i$ Transients

The spatiotemporal characteristics of the first $[Ca^{2+}]_i$ peak from MLO-Y4 and MC3T3-E1 cells were summarized in Figs. 2D–F. The peak magnitudes of both cell types were positively correlated with mechanical stimulation strength (Fig. 2D). When shear stress was lower than 4 Pa, MLO-Y4 cells had significantly higher magnitudes than MC3T3-E1 cells, but no difference was detected for peak magnitudes between two cell types under 4 Pa stimulation. For MLO-Y4 cells, magnitudes of all four groups were significantly different from each other, except between 1 and 2 Pa groups, 2 and 4 Pa groups. The first $[Ca^{2+}]_i$ peak magnitudes of MLO-Y4 cells increased only slightly with shear stress. For MC3T3-E1 cells, the 0.5 and 1 Pa groups had no significant difference, while all other groups were significantly different from each other. For both MLO-Y4 and MC3T3-E1 cells, the time to reach the first $[Ca^{2+}]_i$ peak shortened as the stimulation strength increased (Fig. 2E). The average time for MLO-Y4 cells to reach the first $[Ca^{2+}]_i$ peak was close to 20 seconds. For MC3T3-E1 cells, time to reach first $[Ca^{2+}]_i$ peak was 40 seconds at 0.5 Pa but only 14 seconds at 4 Pa. When fluid shear stress was lower than 4 Pa, MLO-Y4 cells required significantly shorter time to reach the first $[Ca^{2+}]_i$ peak, but vice versa at 4 Pa. It also took shorter time for MLO-Y4 cells to reduce the $[Ca^{2+}]_i$ intensity from peak value to lower level under 0.5, 1, and 2 Pa stimulations (Fig. 2F). No significant difference was detected between the two types of cells at 4 Pa level. A linear regression analysis of the data showed a decreasing trend between relaxation time and stimulation strength for MC3T3-E1 cells, but not for MLO-Y4 cells. ANOVA showed no statistical difference in relaxation time between 1, 2, and 4 Pa groups for MLO-Y4 cells.

The kinetic parameters of the second $[Ca^{2+}]_i$ peaks released by MLO-Y4 and MC3T3-E1 cells were summarized in Fig. 3. The mean values were reported with the exclusion of cells with no $[Ca^{2+}]_i$ peaks or a singular $[Ca^{2+}]_i$ peak. At all stimulation strengths, the MLO-Y4 cells took shorter time than MC3T3-E1 cells to recover from the initial response to release a second $[Ca^{2+}]_i$ peak (Fig. 3A). For both types of cells, the time between first and second $[Ca^{2+}]_i$ peaks decreased as the mechanical stimulation strength increased. The ratio of peak magnitudes ($2^{nd}/1^{st}$) for MLO-Y4 cells ranged between 0.85–0.99 (Fig. 3B), and was not correlated with the magnitude of shear stress. ANOVA further showed that there was no significant difference between all four groups of MLO-Y4 cells. For MC3T3-E1 cells, however, a decreasing trend was detected between the magnitude ratio and stimulation strength. The ratios were 1.07±0.32, 0.88±0.37, 0.72±0.32, and 0.59±0.26 for 0.5, 1, 2, and 4 Pa, respectively. In 2 and 4 Pa groups, the ratio values of MLO-Y4 cells were significantly higher than that of MC3T3-E1 cells, but no significant difference was detected when shear stress was equal to or lower than 1 Pa.

Essential Pathways in $[Ca^{2+}]_i$ Signaling

The essential $[Ca^{2+}]_i$ signaling-related pathways investigated in this study were summarized in Fig. 4A. The average number of $[Ca^{2+}]_i$ peaks of the 16 groups are shown in Fig. 4B. Most inhibitor-treated groups showed significantly less $[Ca^{2+}]_i$ peaks than the untreated or the vehicle control group during the 9-minute fluid low stimulation, except the interrupted PGE_2 pathway for MLO-Y4 cells, which had no significant difference with the vehicle

control group. The suramin treated groups had significantly reduced number of $[Ca^{2+}]_i$ peaks. 79% of MLO-Y4 cells and 60% of MC3T3-E1 cells showed a single $[Ca^{2+}]_i$ peak after the suramin treatment. Depletion of ER calcium stores in both types of cells showed similar effects on $[Ca^{2+}]_i$ signaling. The average number of $[Ca^{2+}]_i$ peaks decreased to one. Thus for both MC3T3-E1 and MLO-Y4 cells, the extracellular ATP pathway and intracellular calcium store are critical for the release of multiple $[Ca^{2+}]_i$ peaks. Blocking GJIC also reduced the number of peaks significantly in both types of cells, but the peak numbers are still significantly higher than the corresponding TG-treated groups. The L-NMMA treatment (NOS blocking) resulted in fewer multiple responses in both cell types. Importantly, the removal of extracellular Ca^{2+} completely abolished the $[Ca^{2+}]_i$ response in both MLO-Y4 and MC3T3-E1 cells. Two-way ANOVA showed that the effects of suramin and LNMMA treatment are dependent on cell types, while the effect of 18α-GA, NS398, and TG are not. Therefore, the purinergic and NO pathways may interact with calcium signaling differently in MLO-Y4 and MC3T3-E1 cells. Again, all MLO-Y4 cells showed more peaks than their corresponding MC3T3-E1 groups, with the exception of the Ca^{2+} free medium group, in which both cell types had no responses.

To confirm the exceptional roles of extracellular Ca^{2+} source in $[Ca^{2+}]_i$ responses, EGTA, a chelating agent of Ca^{2+}, was added into the flow medium during the fluid flow tests after the $[Ca^{2+}]_i$ responses were initiated in cell networks by fluid flow. The oscillations of $[Ca^{2+}]_i$ intensity were immediately stopped by the introduction of EGTA in both types of cells (Fig. 5A). This verified that extracellular Ca^{2+} source was required in $[Ca^{2+}]_i$ signaling for MLO-Y4 and MC3T3-E1 cells during the entire stimulation period.

To explore the potential mechanisms responsible for the difference between MLO-Y4 and MC3T3-E1 cells, we examined the RyR pathway given the critical roles of ER calcium store for multiple $[Ca^{2+}]_i$ responses shown in Fig. 4B. Caffeine (1 mM), an agonist of RyR pathway, was supplied to the flow medium during the fluid flow tests. No dedicated $[Ca^{2+}]_i$ peaks were observed after the supplement of caffeine for either cell type (Fig. 5B). This result was further confirmed by RyR blocking tests on MLO-Y4 cells. RyR, a class of intracellular calcium release channels in the ER that can be activated by millimolar caffeine concentrations, was blocked by 50 μM tetracaine (35). The number of $[Ca^{2+}]_i$ peaks was only slightly reduced in RyR blocked group, although significant (Fig. 5C), and the average peak number of RyR blocked group was 4.0±2.1. To verify the role of PLC-IP_3 pathway in calcium signaling, the osteocytes were treated with neomycin (15 mM) which blocks PLC from hydrolyzing phospholipids into inositol triphosphate (IP_3) and diacylglycerol. The number of $[Ca^{2+}]_i$ peaks in neomycin treated group (1.23±0.57) was much lower than the untreated group (Fig. 5C).

Given the critical roles of ATP pathway in bone cell $[Ca^{2+}]_i$ responses revealed in Fig. 4B and in our previous studies (20,27), we next questioned whether the MLO-Y4 cells released much more ATP into the flow medium under shear stress stimulation, and subsequently whether the high ATP concentration induced more $[Ca^{2+}]_i$ peaks in MLO-Y4 cells. MLO-Y4 cells can release ATP through hemichannels under fluid flow, while MC3T3-E1 cells release ATP mainly through vesicular fusion (53,54). Flow medium was sampled before and post the 9-minute laminar flow stimulations on cell networks. The ATP concentration in medium was measured by using a commercial ATP determination kit (Invitrogen Corporation, Carlsbad, CA). The change of ATP intensity before and post the experiments are reported in Fig. 5D. MC3T3-E1 cells released significantly more ATP into medium under fluid flow than MLO-Y4 cells did. The same result was revealed when the ATP concentration was normalized by the number of cells in cell networks (Fig. 5E).

T-type and L-type VGCCs

A major difference between osteocytes and osteoblasts in calcium signaling is the expression of VGCCs. Osteoblasts predominantly express L-type VGCCs composed of the α_1 pore-forming subunit and several auxiliary subunits. Osteocytes, in contrast, express T-type VGCCs and a small amount of L-type α_1 subunits. Amlodipine (L-type VGCC blocker) induced prolonged declining of $[Ca^{2+}]_i$ in both types of cells (Fig. 6A), which confirmed the existence of L-type VGCC in both osteoblasts and osteocytes and its involvement in calcium signaling. Amlodipine induced an immediate $[Ca^{2+}]_i$ spike in MLO-Y4 cells, but an inversed dive of $[Ca^{2+}]_i$ in MC3T3-E1 cells. The treatment of NNC55-0396 (T-type VGCC blocker) can discontinue the repetitive $[Ca^{2+}]_i$ peaks in MLO-Y4 cells after inducing an immediate spike, and it had no observable effects on MC3T3-E1 cells.

Discussion

Osteocytic network acts as a critical coordinator in bone modeling and remodeling processes. Previous mechanotransduction studies of bone cells were mostly performed on confluent or sub-confluent cell monolayers. However, osteocytes form an elaborate cell network *in vivo*. Each cell connects with several neighboring cells via gap junctions, thereby allowing direct cell-to-cell coupling (55,56). Our previous studies proved that cell-cell communication plays a critical role in determining the characteristics of $[Ca^{2+}]_i$ responses in bone cell networks (20). In this study, the *in vitro* osteocytic network constructed with micro-patterning techniques, for the first time, simulates the *in vivo* bone cell networks in a lacunar-canalicular system.

In this study, unidirectional steady fluid flow was employed as mechanical stimulation on bone cells. Mechanical loading from our daily activities, such as repetitive loading due to locomotion or muscular loading associated with postural control, is presumed to generate oscillatory fluid flow on osteocytes. Previous studies showed that oscillating flow was a much less potent stimulator of bone cells than steady flow (14). To compare the calcium signaling in osteocytes and osteoblasts, steady flow was employed in this study, which could generate distinguishable and prominent difference between two types of cells. Both osteocytes and osteoblasts showed $[Ca^{2+}]_i$ responses when stimulated with laminar steady fluid flow. The responses of osteoblasts, especially those under 2 Pa shear stress, are consistent with those reported in literature (11,12,25). To our knowledge, this is a first study to investigate the flow-induced $[Ca^{2+}]_i$ responses of an osteocytic network. Over 96% of osteocytes showed $[Ca^{2+}]_i$ responses to fluid stimulation, even to flow at low magnitudes (0.5 or 1 Pa shear stress), significantly higher than responsive rate of the osteoblastic cells. Previous studies demonstrated that osteocytes can respond to a pulsatile fluid shear stress as low as 0.5 Pa with a sustained release of PGE_2, but neither osteoblasts nor fibroblasts showed the same response (38). Our new results confirmed that osteocytes are significantly more responsive than osteoblasts under low magnitude fluid flow stimulation. Animal studies have shown that low-intensity mechanical signals incorporate all aspects of a complex remodeling cycle and ultimately stimulate formation of lamellar bone to improve bone quantity and quality (57,58). The unique high sensitivity of osteocytes under low level stimuli revealed in this study may endow the capability of osteocytic networks to act as a dedicated sensor in bone for daily physical activities and to contribute to the entire bone remodeling cycle under low-intensity loading (59).

The spatiotemporal characteristics of $[Ca^{2+}]_i$ transients are also dramatically different in osteocytic and osteoblastic networks. Most osteoblasts release a full $[Ca^{2+}]_i$ peak at the beginning of fluid flow followed by a few weaker peaks, while osteocytes tend to have repetitive $[Ca^{2+}]_i$ peaks with constant magnitudes at a significantly higher number. The spike-like $[Ca^{2+}]_i$ oscillations showed by MLO-Y4 cells can rarely be observed in MC3T3-

E1 cells. The difference is prominent by mere visual inspection. The analysis showed that osteocytes had nearly 100% more $[Ca^{2+}]_i$ peaks than osteoblasts at all levels of stimuli, and the difference aggregates under higher shear stress. Therefore, the highly sensitive osteocytes not only can detect all levels of mechanical signals but also can respond to the signals with unyielding full magnitude $[Ca^{2+}]_i$ spikes.

To identify the mechanisms responsible for the difference between MLO-Y4 and MC3T3-E1 cells in $[Ca^{2+}]_i$ signaling, extensive pathway studies were performed on both types of cell networks. Our previous experiments with osteoblasts showed that the increase of $[Ca^{2+}]_i$ intensity relies on two sources, the influx of extracellular calcium and the release from ER calcium stores (20,27). In present study, both types of cells in calcium-free medium showed no response to fluid flow, which reveals that the $[Ca^{2+}]_i$ transients in both MC3T3-E1 and MLO-Y4 cells induced by mechanical stimulation have to be initiated by extracellular calcium influx. It has been noted that the influx of extracellular calcium is required to evoke the opening of the calcium release channels in the ER of cells (36,60). We further demonstrated that the removal of extracellular calcium source during the fluid flow ceased the $[Ca^{2+}]_i$ responses in MLO-Y4 and MC3T3-E1 cells. Thus, Ca^{2+} in medium is essential for fluid flow induced $[Ca^{2+}]_i$ oscillations in both types of bone cells. The other major calcium source of $[Ca^{2+}]_i$ responses is the intracellular calcium store, which is mainly held within the membrane systems of the ER (61,62). Extracellular ATP can activate the purinergic receptors of the G protein-coupled P_2Y class that activate phospholipase C, resulting in the generation of IP_3 and intracellular calcium release from IP_3-sensitive ER calcium stores. In this study, depletion of the ER stores with thapsigargin or blocking ATP pathway severely hampered multiple $[Ca^{2+}]_i$ spikes in both types of cells. Experiments on MC3T3-E1 monolayer (results not shown) demonstrated that exogenous application of ATP can barely induce $[Ca^{2+}]_i$ responses when the ER Ca^{2+} store was depleted. Besides the ER and ATP pathways, the GJIC, PGE_2 and NO related pathways all showed identical or similar effects on MLO-Y4 and MC3T3-E1 cells. Although these results provide important insight into the $[Ca^{2+}]_i$ signaling mechanisms of MLO-Y4 cells, it is unlikely that one of these pathways is responsible for the dramatic difference between MLO-Y4 and MC3T3-E1 cells.

ATP related pathway is critical for the multiple $[Ca^{2+}]_i$ peaks. Suramin treatment reduced the $[Ca^{2+}]_i$ oscillation to a single peak in both types of bone cells. Our previous study showed that extracellular ATP diffusion plays a critical role in the calcium wave propagation across bone cell networks (20). The ATP release in bone cells can be initiated by mechanically induced Ca^{2+} influx (53,54). However, bioluminescence assay of ATP intensity in extracellular medium showed that MC3T3-E1 cells are releasing more ATP than MLO-Y4 cells upon stimulation. Therefore, the ATP release is the necessary but not sufficient condition for multiple peaks, which is not positively correlated with the amount of ATP released. It is also possible that the P2 family receptors have different expression in two types of cells, and the receptors on MLO-Y4 cells are more sensitive or efficient than those on MC3T3 cells. The results from two-way ANOVA also showed that the effect of suramin treatment is dependent on cell type. We then examined another mechanism related to ER calcium store release, the caffeine-RyR pathway. It has been shown that caffeine can activate intracellular Ca^{2+} release in the osteoclast (60) and enhance the RANKL expression in MC3T3-E1 cells (63). The results showed that neither caffeine stimulation nor the inhibition of RyR can almost completely remove the multiple $[Ca^{2+}]_i$ responses in MLO-Y4 cells, as in suramin or TG treated group.

Once the $[Ca^{2+}]_i$ intensity increases in cells, there is an immediate activation of the processes that restore $[Ca^{2+}]_i$ to resting levels to prevent extended exposure to toxic intensity of $[Ca^{2+}]_i$ (31). This process is achieved by transferring or pumping the Ca^{2+} out of

the cell and back into the ER store simultaneously. Afterwards, the bone cell may be restored or partially restored to its original state before stimulation, ready to release the next $[Ca^{2+}]_i$ response. The $[Ca^{2+}]_i$ transient history in Fig. 2A suggests that the MLO-Y4 cells can fully recover to original state in a short period, while the MC3T3-E1 cells obviously lack this capability. In the recovery process, a lot of ion channels, such as VGCC, store-operated calcium channels, ligand-gated ion channels (*e.g.*, P_2X_7), and the agonists or antagonists acting on these channels may be involved. Previous studies have identified the L-type subunit Cav1.2 as the predominant VGCC pore-forming subunit in osteoblasts (64), while osteocytes express the T-type Cav3.2 subunit (65). These findings were also confirmed in the MC3T3-E1 cell line and the MLO-Y4 cell line (65). Blocking T-type VGCCs stopped the multiple peaks in MLO-Y4 but had no detectable effects on MC3T3-E1 cells. Therefore the T-type VGCC may play an essential role in the unique vigorous $[Ca^{2+}]_i$ responses in MLO-Y4 cells. The physiological roles of T-type channels are very often accomplished by the distinctive low activation threshold of these channels, which boosts up membrane depolarization in excitable cells. The opening of T-type channels allows a Ca^{2+} influx that provokes membrane depolarization and increase in the $[Ca^{2+}]_i$ concentration (66). Understanding the exact cellular and molecular mechanisms responsible for the revealed $[Ca^{2+}]_i$ signaling difference between osteoblasts and osteocytes is beyond the scope of this study, which is another ongoing research area attracting extensive attention.

Bone adapts to mechanical loading in a frequency- and magnitude-dependent fashion. In present study, all the spatiotemporal parameters of first $[Ca^{2+}]_i$ peak in osteoblasts and osteocytes are highly dependent on the strength of mechanical loading. Therefore the physical stimulus information in bone can be encoded in the pattern of $[Ca^{2+}]_i$ signaling in osteocytes. It is well known that the bone cells can memorize and accommodate to mechanical loading history (67). As the mechano-sensory apparatus in bone, osteocytes are conjectured to be the most potent candidate to establish a memory of the local mechanical environment in bone tissue. The high sensitivity of osteocytes and the ability to encode the mechanical stimuli into biochemical signaling found in this study further endowed this hypothesis. Moreover, our pathway studies revealed that the T-type VGCC on osteocytes play an essential role in the kinetics of $[Ca^{2+}]_i$ signaling in osteocytic networks. Interestingly, T-type VGCC exists only in three types of cells, including cardiac cells, neuronal cells, and osteocytes. The cellular function of T-type VGCC in cardiac and neuronal cells includes pacemaking and repetitive firing (66,68). The repetitive $[Ca^{2+}]_i$ peaks in osteocytes revealed in this study resembles the action potentials of a neural network. There is no doubt that osteocytic networks, according to the findings in this study, are qualified to act as an orchestrator of the bone modeling and remodeling process.

Acknowledgments

Funding Sources: This work was supported by NIH grants R21 AR052417, R01 AR052461, and RC1 AR058453 (X. Edward Guo).

We would like acknowledge the contribution of Dr. PuiLeng Isabel Leong for her help in PLC inhibition experiments. We thank Dr. L. Bonewald for her generous gift of MLO-Y4 cells.

References

1. Parfitt AM, Chir B. Cellular Basis of Bone Turnover and Bone Loss -Rebuttal of Osteocytic Resorption-Bone Flow Theory. Clin Orthop Relat Res. 1977; 127:236–247. [PubMed: 912987]
2. Piekarski K, Munro M. Transport Mechanism Operating between Blood-Supply and Osteocytes in Long Bones. Nature. 1977; 269(5623):80–82. [PubMed: 895891]
3. Bonewald LF. Mechanosensation and Transduction in Osteocytes. Bonekey Osteovision. 2006; 3(10):7–15. [PubMed: 17415409]

4. Bonewald LF. The amazing osteocyte. J Bone Miner Res. 2011; 26(2):229–238. [PubMed: 21254230]
5. Tatsumi S, Ishii K, Amizuka N, Li M, Kobayashi T, Kohno K, Ito M, Takeshita S, Ikeda K. Targeted ablation of osteocytes induces osteoporosis with defective mechanotransduction. Cell Metab. 2007; 5(6):464–475. [PubMed: 17550781]
6. Chan ME, Lu XL, Huo B, Baik AD, Chiang V, Guldberg RE, Lu HH, Guo XE. A Trabecular Bone Explant Model of Osteocyte-Osteoblast Co-Culture for Bone Mechanobiology. Cell Mol Bioeng. 2009; 2(3):405–415. [PubMed: 20827376]
7. Kamioka H, Honjo T, Takano-Yamamoto T. A three-dimensional distribution of osteocyte processes revealed by the combination of confocal laser scanning microscopy and differential interference contrast microscopy. Bone. 2001; 28(2):145–149. [PubMed: 11182371]
8. Kamioka H, Ishihara Y, Ris H, Murshid SA, Sugawara Y, Takano-Yamamoto T, Lim SS. Primary cultures of chick osteocytes retain functional gap junctions between osteocytes and between osteocytes and osteoblasts. Microsc Microanal. 2007; 13(2):108–117. [PubMed: 17367550]
9. Hung CT, Pollack SR, Reilly TM, Brighton CT. Real-time calcium response of cultured bone cells to fluid flow. Clin Orthop Relat Res. 1995; (313):256–269. [PubMed: 7641488]
10. Owan I, Burr DB, Turner CH, Qiu J, Tu Y, Onyia JE, Duncan RL. Mechanotransduction in bone: osteoblasts are more responsive to fluid forces than mechanical strain. Am J Physiol. 1997; 273(3 Pt 1):C810–815. [PubMed: 9316399]
11. Donahue SW, Donahue HJ, Jacobs CR. Osteoblastic cells have refractory periods for fluid-flow-induced intracellular calcium oscillations for short bouts of flow and display multiple low-magnitude oscillations during long-term flow. J Biomech. 2003; 36(1):35–43. [PubMed: 12485636]
12. Huo B, Lu XL, Hung CT, Costa KD, Xu QB, Whitesides GM, Guo XE. Fluid Flow Induced Calcium Response in Bone Cell Network. Cell Mol Bioeng. 2008; 1:58–66. [PubMed: 20852730]
13. Tate MLK, Knothe U, Niederer P. Experimental elucidation of mechanical load-induced fluid flow and its potential role in bone metabolism and functional adaptation. Am J Med Sci. 1998; 316(3): 189–195. [PubMed: 9749561]
14. Jacobs CR, Yellowley CE, Davis BR, Zhou Z, Cimbala JM, Donahue HJ. Differential effect of steady versus oscillating flow on bone cells. J Biomech. 1998; 31(11):969–976. [PubMed: 9880053]
15. Rubin J, Rubin C, Jacobs CR. Molecular pathways mediating mechanical signaling in bone. Gene. 2006; 367:1–16. [PubMed: 16361069]
16. Weinbaum S, Cowin SC, Zeng Y. A Model for the Excitation of Osteocytes by Mechanical Loading-Induced Bone Fluid Shear Stresses. J Biomech. 1994; 27(3):339–360. [PubMed: 8051194]
17. Price C, Li W, Novotny JE, Wang LY. An In-Situ Fluorescence-Based Optical Extensometry System for Imaging Mechanically Loaded Bone. J Orthop Res. 2010; 28(6):805–811. [PubMed: 20041487]
18. Adachi T, Aonuma Y, Taira K, Hojo M, Kamioka H. Asymmetric intercellular communication between bone cells: Propagation of the calcium signaling. Biochem Biophys Res Commun. 2009; 389(3):495–500. [PubMed: 19737533]
19. Liu C, Zhao Y, Cheung WY, Gandhi R, Wang LY, You LD. Effects of cyclic hydraulic pressure on osteocytes. Bone. 2010; 46(5):1449–1456. [PubMed: 20149907]
20. Huo B, Lu XL, Costa KD, Xu QB, Guo XE. An ATP-dependent mechanism mediates intercellular calcium signaling in bone cell network under single cell nanoindentation. Cell Calcium. 2010; 47(3):234–241. [PubMed: 20060586]
21. Ajubi NE, Duncan RL. Fluid shear stress increases tyrosine kinase activity in UMR 106.01 cells by a calcium and cytoskeleton dependent process. J Bone Miner Res. 1999; 14:S237–S237.
22. Chen NX, Ryder KD, Pavalko FM, Turner CH, Burr DB, Qiu JY, Duncan RL. Ca^{2+} regulates fluid shear-induced cytoskeletal reorganization and gene expression in osteoblasts. Am J Physiol Cell Physiol. 2000; 278(5):C989–C997. [PubMed: 10794673]
23. You J, Reilly GC, Zhen XC, Yellowley CE, Chen Q, Donahue HJ, Jacobs CR. Osteopontin gene regulation by oscillatory fluid flow via intracellular calcium mobilization and activation of

mitogen-activated protein kinase in MC3T3-E1 osteoblasts. J Biol Chem. 2001; 276(16):13365–13371. [PubMed: 11278573]

24. Ajubi NE, Klein-Nulend J, Alblas MJ, Burger EH, Nijweide PJ. Signal transduction pathways involved in fluid flow-induced PGE_2 production by cultured osteocytes. Am J Physiol Endocrinol Metab. 1999; 276(1):E171–E178.
25. Jorgensen NR, Geist ST, Civitelli R, Steinberg TH. ATP- and gap junction-dependent intercellular calcium signaling in osteoblastic cells. J Cell Biol. 1997; 139(2):497–506. [PubMed: 9334351]
26. Jorgensen NR, Henriksen Z, Brot C, Eriksen EF, Sorensen OH, Civitelli R, Steinberg TH. Human osteoblastic cells propagate intercellular calcium signals by two different mechanisms. J Bone Miner Res. 2000; 15(6):1024–1032. [PubMed: 10841171]
27. Huo B, Lu XL, Guo XE. Intercellular calcium wave propagation in linear and circuit-like bone cell networks. Philos Transact A Math Phys Eng Sci. 2010; 368(1912):617–633. [PubMed: 20047942]
28. Donahue SW, Jacobs CR, Donahue HJ. Flow-induced calcium oscillations in rat osteoblasts are age, loading frequency, and shear stress dependent. Am J Physiol Cell Physiol. 2001; 281(5):C1635–1641. [PubMed: 11600427]
29. Hung CT, Allen FD, Pollack SR, Brighton CT. Intracellular Ca^{2+} stores and extracellular Ca^{2+} are required in the real-time Ca^{2+} response of bone cells experiencing fluid flow. J Biomech. 1996; 29(11):1411–1417. [PubMed: 8894921]
30. Chen NX, Ryder KD, Pavalko FM, Turner CH, Burr DB, Qiu J, Duncan RL. Ca^{2+} regulates fluid shear-induced cytoskeletal reorganization and gene expression in osteoblasts. Am J Physiol Cell Physiol. 2000; 278(5):C989–997. [PubMed: 10794673]
31. Toescu EC. Temporal and Spatial Heterogeneities of Ca^{2+} Signaling -Mechanisms and Physiological Roles. Am J Physiol Gastrointest Liver Physiol. 1995; 32(2):G173–G185.
32. Thompson WR, Majid AS, Czymmek KJ, Ruff AL, Garcia J, Duncan RL, Farach-Carson MC. Association of the a_2d_1 subunit with $Ca_v3.2$ enhances membrane expression and regulates mechanically induced ATP release in MLO-Y4 osteocytes. J Bone Miner Res. 2011
33. Berridge MJ, Lipp P, Bootman MD. The versatility and universality of calcium signalling. Nat Rev Mol Cell Biol. 2000; 1(1):11–21. [PubMed: 11413485]
34. Iqbal J, Zaidi M. Molecular regulation of mechanotransduction. Biochem Biophys Res Commun. 2005; 328(3):751–755. [PubMed: 15694410]
35. Fabiato A. Calcium-induced release of calcium from the cardiac sarcoplasmic reticulum. Am J Physiol. 1983; 245(1):C1–14. [PubMed: 6346892]
36. Mogami H, Tepikin AV, Petersen OH. Termination of cytosolic Ca^{2+} signals: Ca^{2+} reuptake into intracellular stores is regulated by the free Ca^{2+} concentration in the store lumen. Embo J. 1998; 17(2):435–442. [PubMed: 9430635]
37. Norvell SM, Ponik SM, Bowen DK, Gerard R, Pavalko FM. Fluid shear stress induction of COX-2 protein and prostaglandin release in cultured MC3T3-E1 osteoblasts does not require intact microfilaments or microtubules. J Appl Physiol. 2004; 96(3):957–966. [PubMed: 14617531]
38. Kamel MA, Picconi JL, Lara-Castillo N, Johnson ML. Activation of beta-catenin signaling in MLO-Y4 osteocytic cells versus 2T3 osteoblastic cells by fluid flow shear stress and PGE_2: Implications for the study of mechanosensation in bone. Bone. 2010; 47(5):872–881. [PubMed: 20713195]
39. Looms DK, Tritsaris K, Nauntofte B, Dissing S. Nitric oxide and cGMP activate Ca^{2+}-release processes in rat parotid acinar cells. Biochem J. 2001; 355(Pt 1):87–95. [PubMed: 11256952]
40. Volk T, Mading K, Hensel M, Kox WJ. Nitric oxide induces transient Ca^{2+} changes in endothelial cells independent of cGMP. J Cell Physiol. 1997; 172(3):296–305. [PubMed: 9284949]
41. Li N, Sul JY, Haydon PG. A calcium-induced calcium influx factor, nitric oxide, modulates the refilling of calcium stores in astrocytes. J Neurosci. 2003; 23(32):10302–10310. [PubMed: 14614089]
42. Kato Y, Windle JJ, Koop BA, Mundy GR, Bonewald LF. Establishment of an osteocyte-like cell line, MLO-Y4. J Bone Miner Res. 1997; 12(12):2014–2023. [PubMed: 9421234]
43. Guo XE, Takai E, Jiang X, Xu Q, Whitesides GM, Yardley JT, Hung CT, Chow EM, Hantschel T, Costa KD. Intracellular calcium waves in bone cell networks under single cell nanoindentation. Mol Cell Biomech. 2006; 3(3):95–107. [PubMed: 17263256]

44. Singhvi R, Kumar A, Lopez GP, Stephanopoulos GN, Wang DI, Whitesides GM, Ingber DE. Engineering cell shape and function. Science. 1994; 264(5159):696–698. [PubMed: 8171320]
45. Godin LM, Suzuki S, Jacobs CR, Donahue HJ, Donahue SW. Mechanically induced intracellular calcium waves in osteoblasts demonstrate calcium fingerprints in bone cell mechanotransduction. Biomech Model Mechanobiol. 2007; 6(6):391–398. [PubMed: 17082961]
46. Hung CT, Allen FD, Mansfield KD, Shapiro IM. Extracellular ATP modulates $[Ca^{2+}]_i$ in retinoic acid-treated embryonic chondrocytes. Am J Physiol. 1997; 272(5 Pt 1):C1611–1617. [PubMed: 9176153]
47. Ralston SH, Todd D, Helfrich M, Benjamin N, Grabowski PS. Human osteoblast-like cells produce nitric oxide and express inducible nitric oxide synthase. Endocrinology. 1994; 135(1):330–336. [PubMed: 7516867]
48. Guo Y, Martinez-Williams C, Gilbert KA, Rannels DE. Inhibition of gap junction communication in alveolar epithelial cells by 18a-glycyrrhetinic acid. Am J Physiol. 1999; 276(6 Pt 1):L1018–1026. [PubMed: 10362727]
49. Yellowley CE, Li Z, Zhou Z, Jacobs CR, Donahue HJ. Functional gap junctions between osteocytic and osteoblastic cells. J Bone Miner Res. 2000; 15(2):209–217. [PubMed: 10703922]
50. Yellowley CE, Jacobs CR, Donahue HJ. Mechanisms contributing to fluid-flow-induced Ca^{2+} mobilization in articular chondrocytes. J Cell Physiol. 1999; 180(3):402–408. [PubMed: 10430180]
51. Huang L, Keyser BM, Tagmose TM, Hansen JB, Taylor JT, Zhuang H, Zhang M, Ragsdale DS, Li M. NNC 55-0396 [(1S,2S)-2-(2-(N-[(3-benzimidazol-2-yl)propyl]-N-methylamino)ethyl)-6-fluoro-1,2,3,4-tetrahydro-1-isopropyl-2-naphtyl cyclopropanecarboxylate dihydrochloride]: a new selective inhibitor of T-type calcium channels. J Pharmacol Exp Ther. 2004; 309(1):193–199. [PubMed: 14718587]
52. Yoshida J, Ishibashi T, Nishio M. Antiproliferative effect of Ca^{2+} channel blockers on human epidermoid carcinoma A431 cells. Eur J Pharmacol. 2003; 472(1–2):23–31. [PubMed: 12860469]
53. Genetos DC, Geist DJ, Liu D, Donahue HJ, Duncan RL. Fluid shear-induced ATP secretion mediates prostaglandin release in MC3T3-E1 osteoblasts. J Bone Miner Res. 2005; 20(1):41–49. [PubMed: 15619668]
54. Genetos DC, Kephart CJ, Zhang Y, Yellowley CE, Donahue HJ. Oscillating fluid flow activation of gap junction hemichannels induces ATP release from MLO-Y4 osteocytes. J Cell Physiol. 2007; 212(1):207–214. [PubMed: 17301958]
55. Doty SB. Morphological Evidence of Gap-Junctions between Bone-Cells. Calcif Tissue Int. 1981; 33(5):509–512. [PubMed: 6797704]
56. Donahue HJ, McLeod KJ, Rubin CT, Andersen J, Grine EA, Hertzberg EL, Brink PR. Cell-to-cell communication in osteoblastic networks: cell line-dependent hormonal regulation of gap junction function. J Bone Miner Res. 1995; 10(6):881–889. [PubMed: 7572312]
57. Rubin C, Turner AS, Bain S, Mallinckrodt C, McLeod K. Anabolism - Low mechanical signals strengthen long bones. Nature. 2001; 412(6847):603–604. [PubMed: 11493908]
58. Rubin C, Turner AS, Muller R, Mittra E, McLeod K, Lin W, Qin YX. Quantity and quality of trabecular bone in the femur are enhanced by a strongly anabolic, noninvasive mechanical intervention. J Bone Miner Res. 2002; 17(2):349–357. [PubMed: 11811566]
59. Turner CH, Forwood MR, Otter MW. Mechanotransduction in Bone: Do Bone Cells Act as Sensors of Fluid Flow. Faseb Journal. 1994; 8(11):875–878. [PubMed: 8070637]
60. Shankar VS, Pazianas M, Huang CL, Simon B, Adebanjo OA, Zaidi M. Caffeine modulates Ca^{2+} receptor activation in isolated rat osteoclasts and induces intracellular Ca^{2+} release. Am J Physiol. 1995; 268(3 Pt 2):F447–454. [PubMed: 7900844]
61. Berridge MJ. Inositol trisphosphate and calcium signalling. Nature. 1993; 361(6410):315–325. [PubMed: 8381210]
62. Clapham DE. Calcium signaling. Cell. 1995; 80(2):259–268. [PubMed: 7834745]
63. Liu SH, Chen C, Yang RS, Yen YP, Yang YT, Tsai C. Caffeine enhances osteoclast differentiation from bone marrow hematopoietic cells and reduces bone mineral density in growing rats. J Orthop Res. 2011; 29(6):954–960. [PubMed: 21284030]

64. Ryder KD, Duncan RL. Parathyroid hormone enhances fluid shear-induced $[Ca^{2+}]_i$ signaling in osteoblastic cells through activation of mechanosensitive and voltage-sensitive Ca^{2+} channels. J Bone Miner Res. 2001; 16(2):240–248. [PubMed: 11204424]

65. Shao Y, Alicknavitch M, Farach-Carson MC. Expression of voltage sensitive calcium channel (VSCC) L-type $Ca_V1.2$ (a1C) and T-type $Ca_V3.2$ (a1H) subunits during mouse bone development. Dev Dyn. 2005; 234(1):54–62. [PubMed: 16059921]

66. Nilius B, Talavera K, Verkhratsky A. T-type calcium channels: The never ending story. Cell Calcium. 2006; 40(2):81–88. [PubMed: 16797069]

67. Turner CH, Robling AG, Duncan RL, Burr DB. Do bone cells behave like a neuronal network? Calcif Tissue Int. 2002; 70(6):435–442. [PubMed: 12149636]

68. Talavera K, Nilius B. Biophysics and structure-function relationship of T-type Ca^{2+} channels. Cell Calcium. 2006; 40(2):97–114. [PubMed: 16777221]

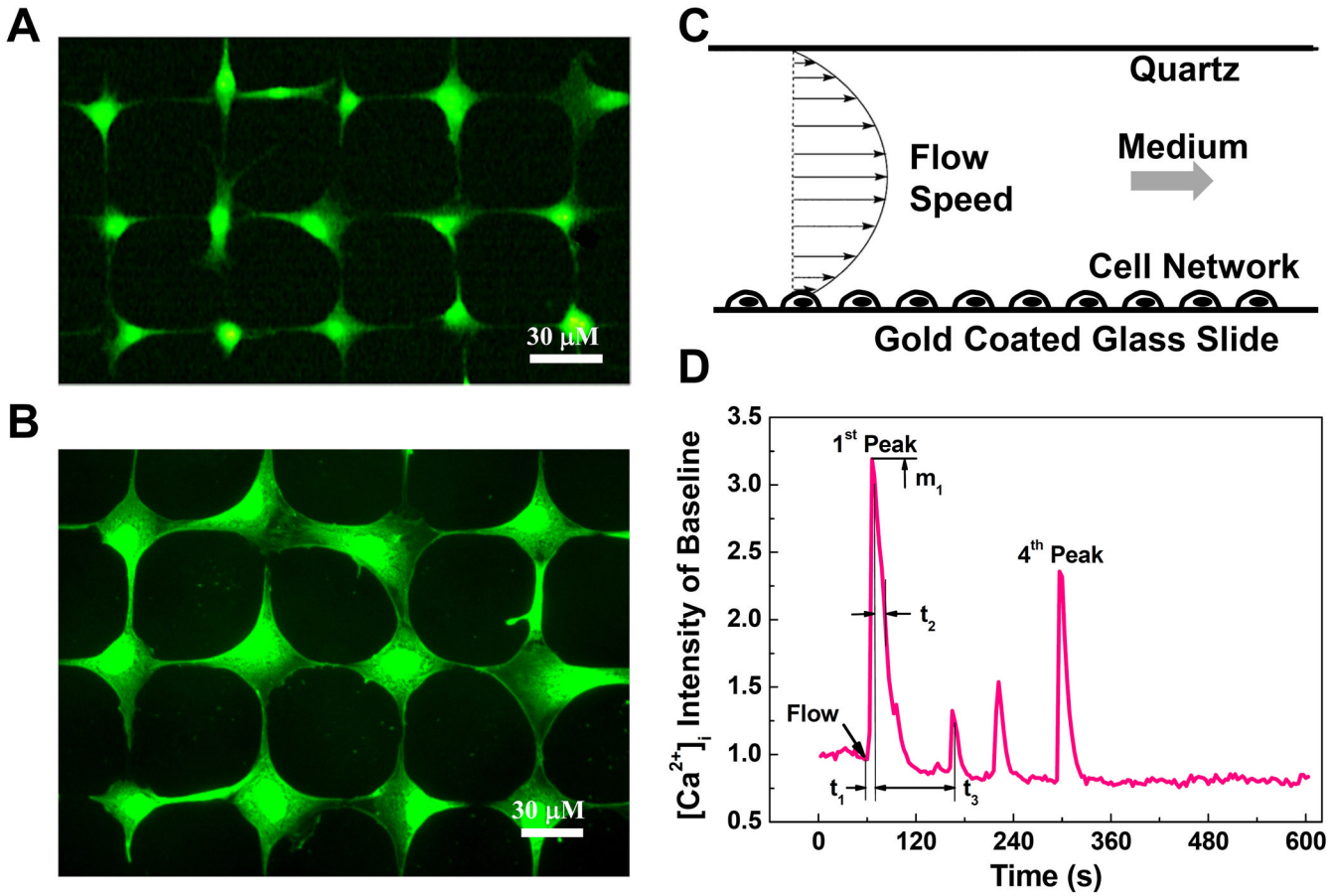

Figure 1.

Micro-patterned bone cell networks, laminar fluid flow stimulation, and the definition of spatiotemporal parameters to characterize the $[Ca^{2+}]_i$ transients. Fluorescent images show typical well-formed (A) MLO-Y4 and (B) MC3T3-E1 cell networks. The cells were loaded with Fura-2 AM to indicate intracellular calcium ions. Each cell attaches on a round island on micro-patterned slides. The island is 15 μm in diameter for MLO-Y4 and 20 μm for MC3T3-E cells. Scale bars in both images are 30 μm. (C) The slide with patterned cell network was mounted in a laminar fluid flow chamber. The laminar flow rate was controlled by a high-resolution magnetic gear pump to generate 0.5, 1, 2, or 4 Pa shear stress on the cell surface. (D) The calcium responses of cell networks were recorded for ten minutes: one minute for baseline and nine minutes during fluid flow stimulation. The $[Ca^{2+}]_i$ intensity was represented by averaging image intensity inside a normalized cell over baseline level. Number of $[Ca^{2+}]_i$ peaks, magnitude of 1st peak m_1, time to 1st peak t_1, relaxation time of 1st peak t_2, and time interval between 1st and 2nd peaks t_3 were defined here using a typical $[Ca^{2+}]_i$ transient of MC3T3-E1 cell.

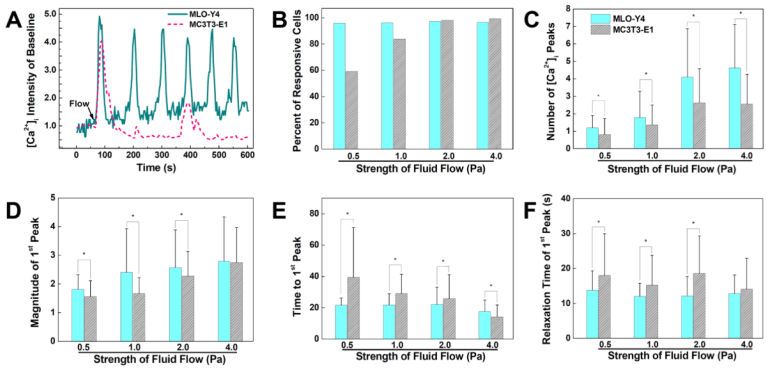

Figure 2.

Comparison of $[Ca^{2+}]_i$ responses of MLO-Y4 and MC3T3-E1 cells under fluid flow stimulations, and the spatiotemporal characterization of the 1st $[Ca^{2+}]_i$ peaks released by MLO-Y4 and MC3T3-E1 cells. (A) Typical $[Ca^{2+}]_i$ transients of a MLO-Y4 cell and a MC3T3-E1 cell under 2 Pa shear stress stimulation. (B) The number of responsive MLO-Y4 and MC3T3-E1 cells under four different fluid flow strengths. (C) Number of peaks in $[Ca^{2+}]_i$ responses during 9-minute fluid flow stimulation. (D) Magnitude of 1st peak in $[Ca^{2+}]_i$ responses. (E) Time to reach the 1st $[Ca^{2+}]_i$ peak since the onset of fluid flow. (F) Relaxation time for $[Ca^{2+}]_i$ intensity to drop 50% from peak magnitude. Data shown are mean ± std dev. * = statistically significant difference between two types of cells at a specific fluid flow strength, $P<0.05$.

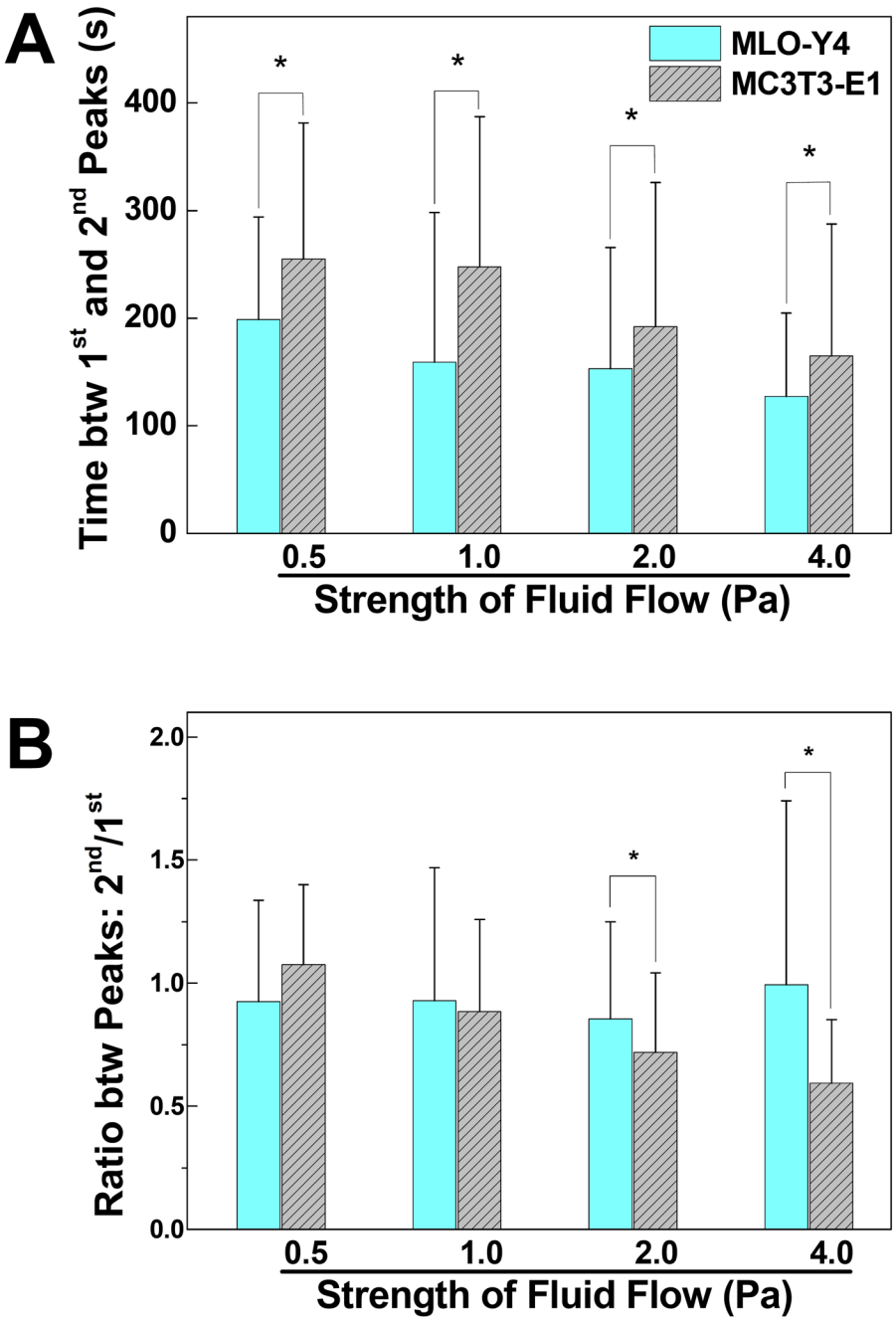

Figure 3.

Comparison of the spatiotemporal characterization of the 2nd peaks in $[Ca^{2+}]_i$ responses. Only cells with more than one $[Ca^{2+}]_i$ peak were counted. (A) Time gap between the highest magnitudes of the 1st and 2nd $[Ca^{2+}]_i$ peaks. (B) The magnitude ratio between 2nd and 1st $[Ca^{2+}]_i$ peaks. Data shown are mean ± std dev. * = statistically significant difference between two types of cells at a specific fluid flow strength, $P<0.05$.

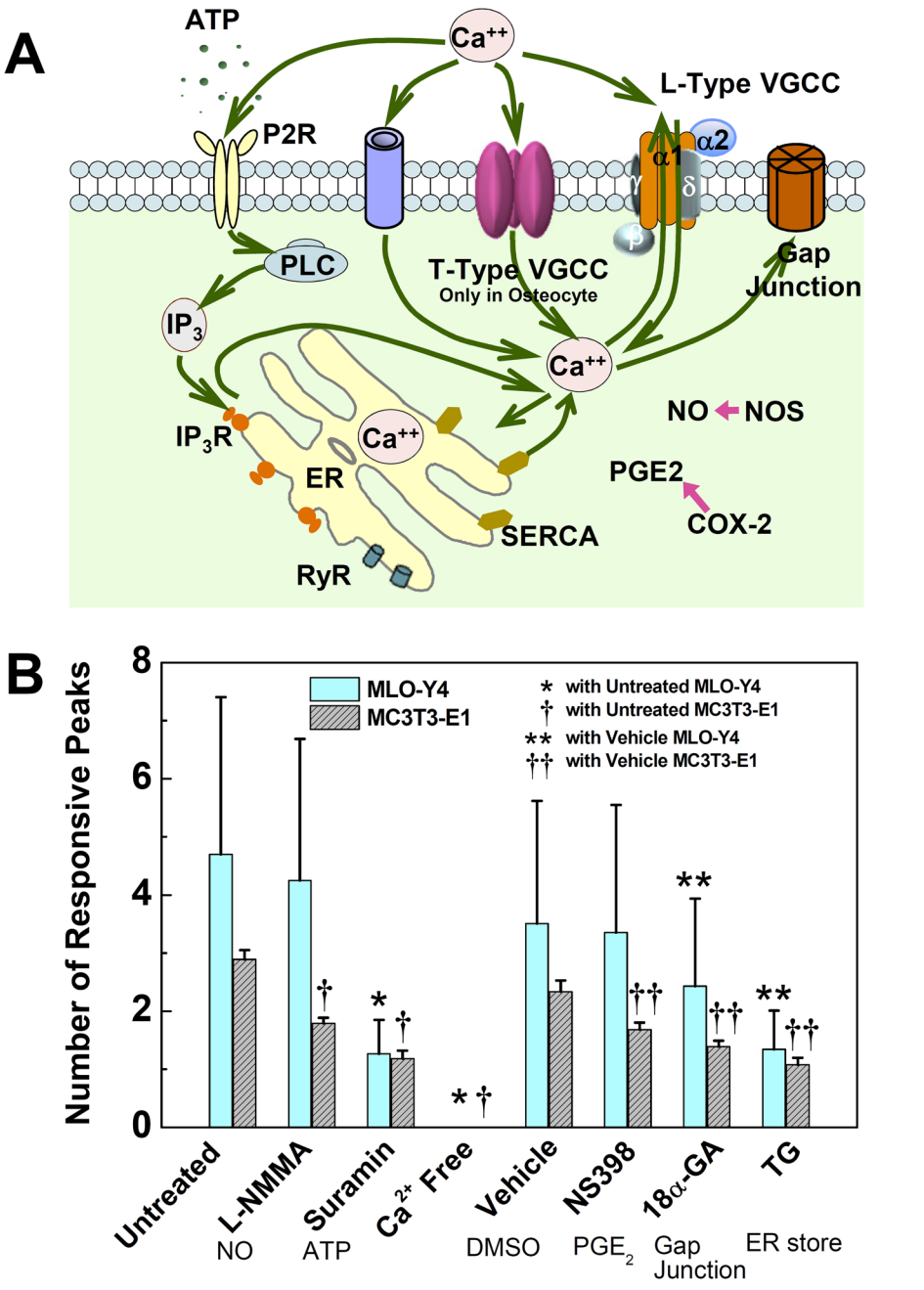

Figure 4.

Roles of critical signaling pathways involved in $[Ca^{2+}]_i$ responses were examined and compared between MLO-Y4 and MC3T3-E1 cells. (A) A schematic drawing of calcium signaling pathways in bone cells investigated in present study. The cytoplasm calcium can exchange with extracellular calcium source in medium and intracellular calcium store in ER. Voltage gated calcium channels, ligand gated ion channels (*e.g.*, ATP activated P_2X_7), G-protein and stretch-gated ion channels can transfer Ca^{2+} between intra- and extracellular environments. Gap junction provides a direct channel for small molecule (*e.g.*, IP_3 and Ca^{2+}) diffusion between connected neighboring cells. The calcium store in ER can be released by activation of IP_3 or ryanodine receptors on ER membrane. As two of the most

essential signaling pathways involved in bone cell metabolisms, PGE_2 and NO pathways were also investigated to identify their correlations with $[Ca^{2+}]_i$ responses under mechanical stimulation. (B) The average number of responsive $[Ca^{2+}]_i$ peaks from pharmacologically pretreated groups. The affected pathways are listed below the corresponding chemicals. L-NMMA (MLO-Y4: 4.2±2.4; MC3T3: 1.8±0.1), Suramin (MLO-Y4: 1.3±0.6; MC3T3: 1.2±0.1) and Ca^{2+} free medium (MLO-Y4: 0; MC3T3, 0) treated groups were compared with untreated group (MLO-Y4: 4.7±2.7; MC3T3: 2.9±0.2). NS398 (MLO-Y4: 3.4±2.2; MC3T3: 1.7±0.1), 18α-GA (MLO-Y4: 2.4±1.5; MC3T3: 1.4±0.1) and Thapsigargin (MLO-Y4: 1.3±0.7; MC3T3: 1.1±0.1) treated groups were compared with DMSO vehicle control group (MLO-Y4: 3.5±2.1; MC3T3: 2.3±0.2). The group of Ca^{2+} free medium had no response to fluid flow. ($P < 0.05$. Data shown are mean ± std dev.)

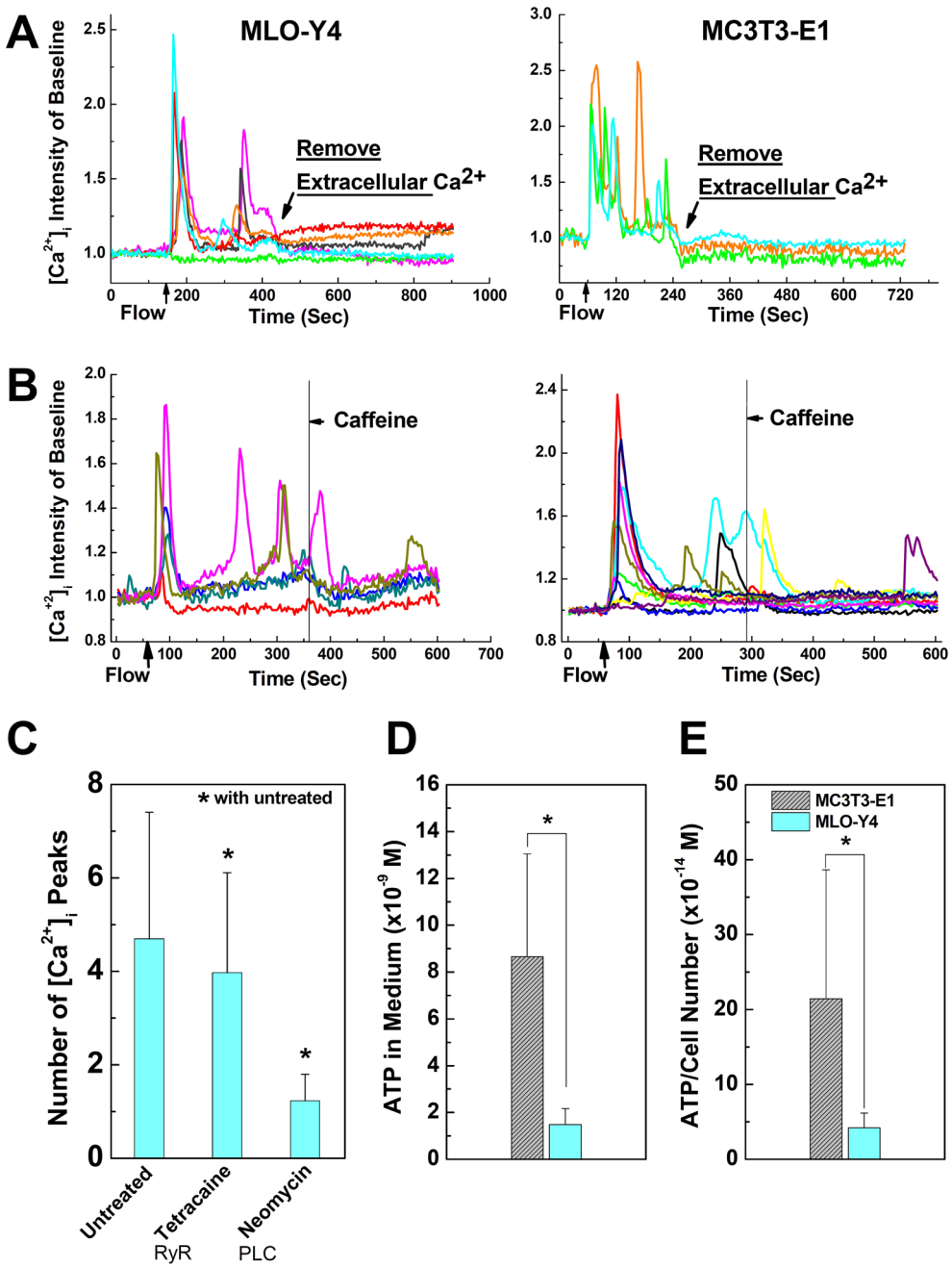

Figure 5.

Roles of extracellular calcium source and caffeine in $[Ca^{2+}]_i$ responses of MLO-Y4 (left) and MC3T3-E1 (right) cells. (A) Depletion of extracellular calcium in medium during the fluid flow stimulation terminates the $[Ca^{2+}]_i$ responses in both MLO-Y4 and MC3T3-E1 cells. (B) Adding caffeine in medium during fluid flow stimulation has no significant effect on the $[Ca^{2+}]_i$ responses in either MLO-Y4 or MC3T3-E1 cells based on visual inspection. (C) The average number of responsive $[Ca^{2+}]_i$ peaks in MLO-Y4 cells when treated with RyR inhibitor and PLC pathway inhibitor. (D) The ATP concentration in flow medium after fluid flow stimulation on MLO-Y4 or MC3T3-E1 cells. (E) ATP concentration in flow

medium showing in (D) normalized by corresponding cell numbers. Data shown are mean ± std dev.

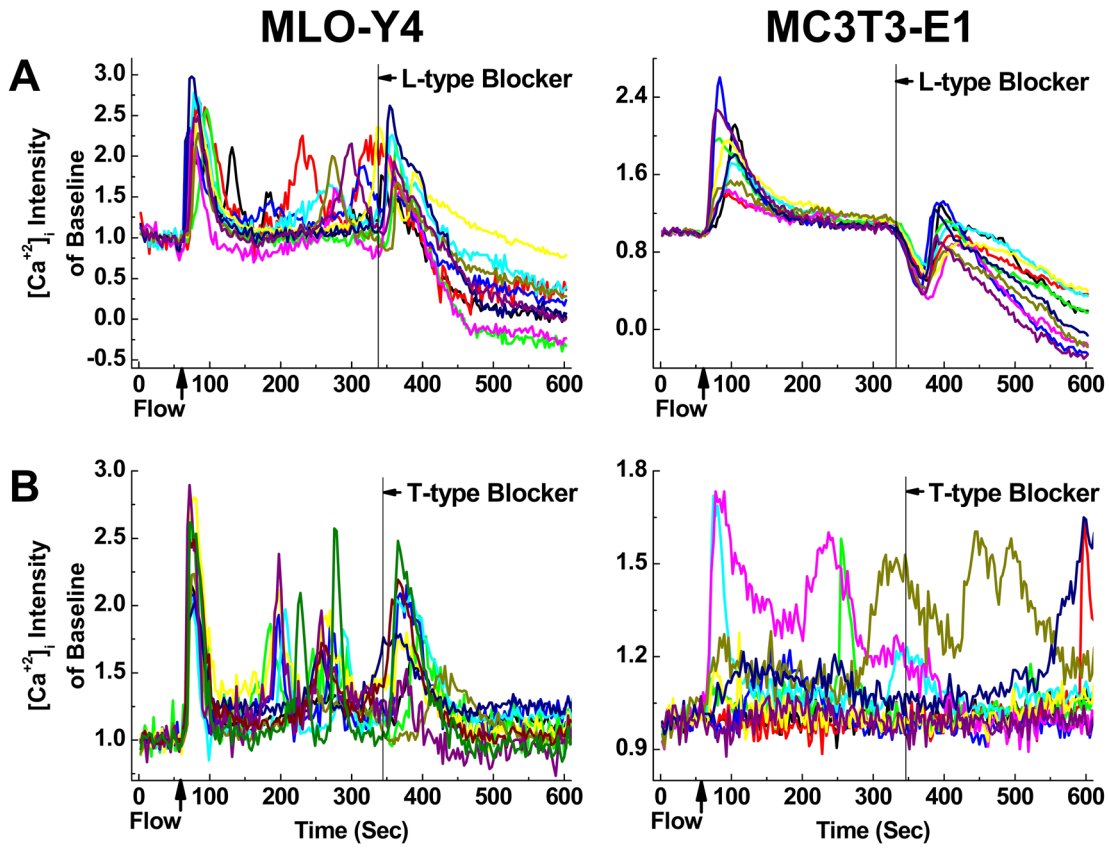

Figure 6.

The effect of L-type (A) and T-type (B) VGCC blockers on $[Ca^{2+}]_i$ transients in MLO-Y4 and MC3T3-E1 cell networks during fluid flow stimulation. The chemicals reached the cell networks at 340th second. $[Ca^{2+}]_i$ responses from 10 cells were plotted in each figure.

Table 1

Number of cell networks (slides) and analyzed cells in different experimental groups.

Shear Stress (Pa)		**5**	**10**	**20**	**40**
MLO-Y4	**Slides**	3	4	4	5
	cells	150	440	355	370
MC3T3-E1	**slides**	3	3	7	4
	cells	130	124	420	259